Large magnetocaloric effect in sintered ferromagnetic EuS

Large magnetocaloric effect in sintered ferromagnetic EuS

Koichi Matsumoto[a,*], Liang Li[b], Shinji Hirai[b], Eiji Nakamura[b], Daiki Murayama[a], Yutaro Ura[a], Satoshi Abe[a]

[a]*Department of Physics, Kanazawa University, Kanazawa 920-1192, Japan*
[b]*Department of Materials Science and Engineering, Muroran Institute of Technology, Muroran 050-8585, Japan*

Abstract

We present magnetocaloric effect measurements of the ferromagnetic semiconductor EuS in the vicinity of its ordering temperature. Single phase EuS powder was synthesized by CS_2 gas sulfurization of Eu_2O_3. A sintered compact with relative density over 95% was prepared by pulsed electric current sintering of the powder. Temperature and magnetic field dependence of the magnetization and specific heat were characteristic of a paramagnetic to ferromagnetic second order phase transition. The entropy change induced by an external magnetic field and the specific heat were both close to those of a single crystal. We obtained an entropy-temperature (S–T) diagram of the EuS sintered compact. Carnot cycle liquefaction of hydrogen using EuS was compared with several other materials, with results indicating that sintered EuS is an excellent magnetic refrigerant for hydrogen liquefaction.

Keywords: Magnetocaloric Material, Entropy, Magnetic Refrigeration, Hydrogen, Liquefaction

1. Introduction

Refrigeration using the magnetocaloric effect (MCE) has a long history. Debye [1] in 1926 and Giauque [2] in 1927 described the theoretical basis of adiabatic demagnetization cooling. Because of the reversibility of entropy

*Corresponding author. E-mail address: k.matsu@staff.kanazawa-u.ac.jp

changes, magnetic refrigeration can achieve a very high thermodynamic efficiency. Magnetic refrigeration systems can be environmentally friendly, quiet, and potentially more efficient than conventional gas expansion systems. A further advantage of magnetic refrigeration is its use of solid magnetic materials, which have typically 1000 times higher entropy density than gases. MCE-based magnetic refrigerators can operate over a wide temperature range, from room temperature to microkelvins. In recent years, magnetic refrigeration research has been expanded to various applications such as space cryogenics [3], hydrogen liquefaction [4] and room temperature refrigerators [5, 6]. Magnetic materials with large MCE have been studied extensively [7, 8].

Hydrogen is one of the cleanest energy resources and is also a useful cryogenic refrigerant for superconducting technologies operating above 20 K. Denser liquid hydrogen has a great advantage over gaseous hydrogen for storage and transportation, but its use critically depends on highly efficient liquefaction methods and adiabatic storage because of 20.3 K boiling point at 1 atmosphere.

One of the authors, KM developed a hydrogen magnetic refrigeration system that consisted of a Carnot cycle liquefaction stage and an active magnetic regenerator (AMR) cycle for the precooling stages [4]. In the Carnot cycle, over 80% liquefaction efficiency was achieved using Dy-substituted gadolinium aluminum garnet ($(Dy_xGd_{1-x})_3Al_5O_{12}$, DGAG) [4, 9]. The MCE in a series of Fe-modified gadolinium gallium garnets ($Gd_3(Ga_{1-x}Fe_x)_5O_{12}$, GGIG) was studied, which demonstrated that GGIGs have a larger entropy change ΔS than gadolinium gallium garnet ($Gd_3Ga_5O_{12}$, GGG) around 20 K [10, 11]. RM_2 (R= rare earth, M= Al, Ni, or Co) compounds have large entropy changes and magnetic transition temperatures can be controlled by varying R and/or M so that these compounds have good potential as magnetic refrigerators for hydrogen liquefaction [12, 13, 14, 15].

In europium monochalcogenides, the divalent europium ion has a $4f^7$ electron configuration, an electronic S-state with total spin angular momentum of 7/2 [16]. The crystalline electric field effect and magnetic anisotropy in this system are expected to be small. This electronic character of europium monochalcogenides should produce a large and isotropic MCE. EuS is a ferromagnetic semiconductor with a NaCl crystal structure having a second order phase transition from ferromagnetic to paramagnetic at $T_C \sim 18$ K [16]. As this temperature is near the boiling point of hydrogen, EuS is a potential magnetic refrigeration material. Investigations of other europium monochalcogenides such as EuSe [17] and EuO [18] showed a first order mag-

netic transition from paramagnetic to antiferromagnetic at $T_N \sim 4.6$ K and a second order magnetic transition from paramagnetic to ferromagnetic at $T_C \sim 69$ K, respectively.

In EuS, theoretical studies [19, 20, 21] have suggested significant ΔS. Experimental observation of the MCE was first reported by Bredy and Seyfert [22], who used a flat sintered polycrystalline EuS sample and measured ΔS up to 3 T. Their observed ΔS were much smaller than those expected from theoretical calculations. Recently, the MCE was studied in a single crystal of EuS grown by the Bridgman method [23]. Magnetization and specific heat were measured at magnetic fields up to 5 T applied along the [100] and [110] directions. A large and isotropic MCE without hysteresis loss was observed. These experiments suggest that the degree of crystalline quality is important to obtain useful high MCE in EuS.

Polycrystalline materials that can be manufactured into shapes such as plates or spheres are necessary for practical use of magnetic materials in a magnetic refrigerator. Moreover, the MCE of the polycrystal must be large, comparable to a single crystal. We have succeeded in manufacturing a sintered EuS polycrystal compact that has a relative density over 95%. In this paper, we report that the MCE of this sintered polycrystal is close to that of a single crystal and is a good candidate material for magnetic refrigeration.

2. Experimental Procedures

A sintered compact was prepared by pulsed electric current sintering of single phase EuS powder, which was synthesized by CS_2 gas sulfurization of Eu_2O_3. In the CS_2 gas sulfurization, a quartz board containing Eu_2O_3 powder was inserted into a reaction tube which was heated in an Ar atmosphere. CS_2 gas was introduced into the tube using Ar as the carrier. The product, single phase EuS, was confirmed by X-ray diffraction. Subsequently, the synthesized powder was filled into a graphite die and sintered at 1873 K in vacuum under high pressure using a pulsed electric current sintering apparatus. Details of the synthesizing process will be reported elsewhere [24].

Density of the sintered compact was determined as 5.46 g/cm^3 (95% of that for a single crystal) by Archimedes method. Magnetization M was measured using a commercial SQUID magnetometer (MPMS, Quantum Design) at discrete intervals of magnetic field between 0.01 and 5 T. A thermal

relaxation method was used to measure specific heat C as a function of temperature at various magnetic fields from 0 to 5 T using a physical properties measurement system (PPMS, Quantum Design).

3. Results

3.1. Magnetization

In the upper panel of Fig. 1, M for sintered EuS is shown as functions of temperature in magnetic fields up to 5 T. In any constant field, M decreased with increasing temperature above 2 K. M tended to saturate at about 3.9×10^4 emu/mol at low temperatures. This corresponds to 7 $\mu_{\rm B}$ per Eu atom, which is expected for $g=2$ and $J=S=7/2$ in the $4f^7$ electron configuration.

The lower panel of Fig. 1 shows M and inverse susceptibility at 100 Oe between 2 and 300 K. M shows a paramagnetic to ferromagnetic transition at the Curie temperature $T_{\rm C}=16.5$ K. Above $T_{\rm C}$, $M(T)$ is described by the Curie-Weiss law. The paramagnetic Curie temperature $\theta=17$ K and the effective magnetic moment $\mu_{\rm eff}=7.2$ $\mu_{\rm B}$ are obtained from this plot. The $\mu_{\rm eff}$ of sintered EuS is slightly less than the 7.9 $\mu_{\rm B}$ for single crystal EuS [23].

The magnetic entropy change ΔS was calculated from the magnetization using Maxwell's relation,

$$\Delta S(T,H)=\int_0^H\left(\frac{\partial M}{\partial T}\right)_H dH, \tag{1}$$

where H is the applied magnetic field. Figure 2 shows the obtained $-\Delta S$ of our sintered EuS. The $-\Delta S$ curve has a caret-like shape. For a given magnetic field, it increases with temperature below $T_{\rm C}$, has a peak $-\Delta S_{\rm max}$ at 17.5 K and decreases with temperature above this. The form of these results is identical to single crystal data, and the peak temperatures are very close to each other, but the magnitude of the molar entropy change $-\Delta S$ for our sintered sample was about 5% smaller than that for a single crystal [23]. The maximum entropy change $-\Delta S_{\rm max}$ for 5 T corresponds to 36% of the maximum magnetic entropy $R\ln(2S+1)$ with $S=7/2$. We discuss details of ΔS in section 4.

3.2. Specific heat

The specific heat C for sintered EuS is shown in Fig. 3. C in zero field has a λ-shaped temperature dependence and a sharp peak at 16.5 K. On

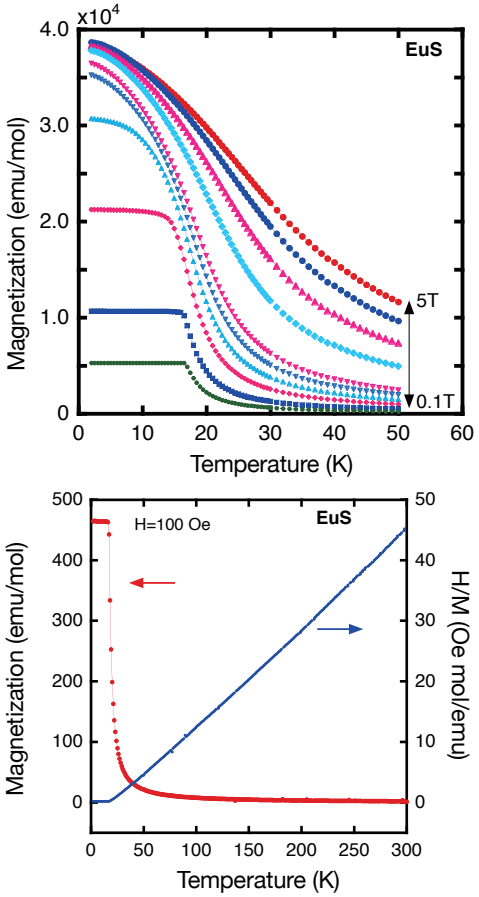

Figure 1: (Upper panel) Magnetization of sintered EuS as functions of temperature in magnetic fields of 0.1, 0.2, 0.4, 0.6, 0.8, 1, 2, 3, 4, and 5 T. (Lower panel) Magnetization and inverse susceptibility of sintered EuS at 100 Oe versus temperature.

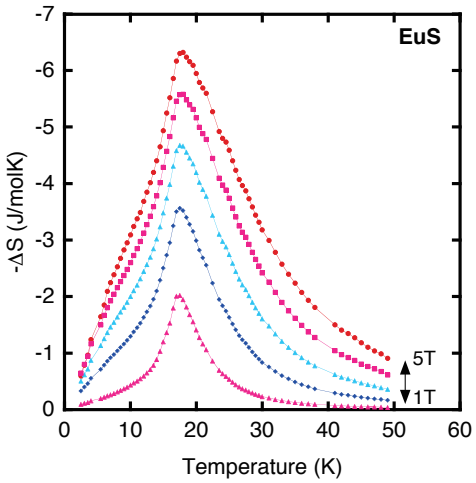

Figure 2: Entropy change $-\Delta S$ of sintered EuS as functions of temperature in magnetic fields of 1, 2, 3, 4, and 5 T.

application of a magnetic field, the specific heat peak becomes broader and shifts to a higher temperature with increasing magnetic field. In 5 T field, specific heat peak is almost smeared. This temperature and magnetic field dependence is typical for magnetic materials with second order phase transitions from ferromagnetic to paramagnetic states. The $C(T, H)$ curves are almost identical to those for single crystal EuS [23].

3.3. Evaluation of Entropy

The total entropy S was obtained by integrating C/T over temperatures from 0 to T at constant magnetic field, as

$$S(T, H) = \int_0^T \left(\frac{C(T, H)}{T} \right)_H dT, \tag{2}$$

where $C(T, H)$ is the specific heat at a constant field H. $S(T, H)$ of sintered EuS were calculated from the data using the above equation. Figure 4 gives the entropy-temperature diagram (S–T) of sintered EuS. The entropy at 0 T and just above T_C is close to $R\ln(8)$. This indicates that most of the spin entropy of the $S = 7/2$ state is released at T_C. As shown in Fig. 4, entropy S of sintered EuS is notably reduced by magnetic field between 10 and 30 K, which corresponds to $-\Delta S$ in Fig. 2. This holds promise for its use as a magnetic refrigerant near the hydrogen liquefaction point.

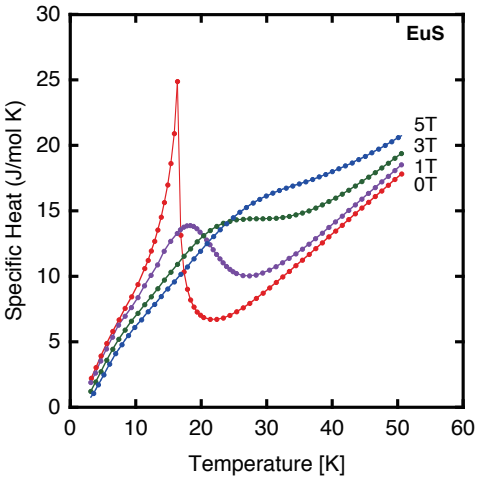

Figure 3: Specific heat C of sintered EuS as functions of temperature in magnetic fields of 0, 1, 3, and 5 T.

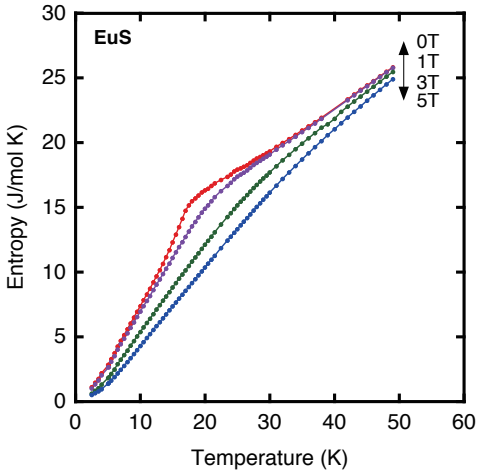

Figure 4: Entropy $S(T, H)$ of sintered EuS as functions of temperature in magnetic fields of 0, 1, 3, and 5 T.

4. Discussion

Maximum entropy change $-\Delta S_{\max}$ at each field strength and relative cooling power (RCP) are often used in order to compare the MCE among various materials [25, 26]. The parameter RCP is defined as $|\Delta S|\,\delta_{\mathrm{FWHM}}$, where δ_{FWHM} is the full width at half maximum of $-\Delta S_{\max}$ in temperature [25, 26]. The MCE of single crystal EuS has been compared against various materials that have transition temperatures around 20 K using $-\Delta S_{\max}$ and RCP in Ref. [23]. It has been noted that EuS shows good potential as a magnetic refrigerant.

Comparing the maximum entropy change $-\Delta S_{\max}$ of our sintered EuS to those of the polycrystal studied by Bredy and Seyfert [22] and the single crystal EuS [23], Fig. 5 shows the values of $-\Delta S_{\max}$ per cubic centimeter. It is important to compare using volumetric entropy change because relative density and the MCE depend on the synthesizing process. $-\Delta S_{\max}$ does not become saturated in a 5 T field. The $-\Delta S_{\max}$ per cubic centimeter of our sample is about 10% smaller than that of the single crystal [23], assumed to have a relative density of 100% for single crystal. Our sintered EuS has about 20% larger $-\Delta S_{\max}$ than that of Bredy and Seyfert [22], whereas the relative density of our sample is 95% compared with 89% for the Bredy and Seyfert sample [22]. Yet the difference in $-\Delta S_{\max}$ between the two sintered samples is much larger than the difference in relative density. We ascribe the larger $-\Delta S_{\max}$ of our sintered sample to higher quality. MCE is known to be affected by inhomogeneity, impurity phases, lattice defects, and so on. In our sintered compact, only tiny amounts of oxygen and carbon were detected by composition analysis. No information was given about impurity in the single crystal in Ref. [23] and the polycrystal by Bredy and Seyfert [22]. It is impractical to use a single crystal in magnetic refrigerators unless large single crystals can be manufactured inexpensively. Sintered polycrystals represent a feasible technology because of processability and cost. We are improving our synthesizing process so that higher than 95% relative density sintered compacts can be made [24].

S–T diagrams are indispensable to analyze thermal cycles. We reviewed the S–T diagram of our sintered EuS in section 3. Here we will evaluate and compare the Carnot cycle operating with EuS and several garnet materials and RM_2 compounds with T_{C} near 20 K. Due to the limited available volume in high magnetic field applications, it is useful to compare cycles in volumetric entropy. In this comparison, we use densities calculated from

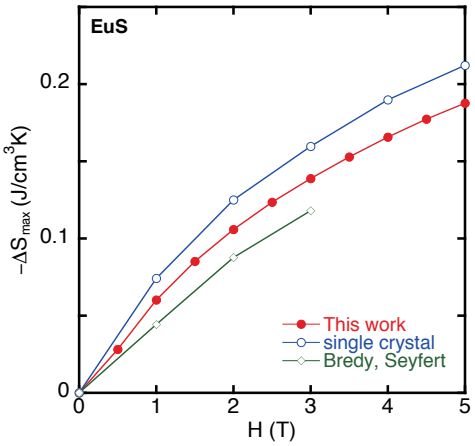

Figure 5: Maximum differential entropy $-\Delta S_{\max}$ of sintered compacts and single crystal EuS induced by several magnetic fields. Density ρ =5.75 g/cm^3 is used to convert the single crystal data.

crystallographic data because densities of other materials are not always reported in MCE measurements. The absorbed heat at 20 K per unit volume $Q_{20\mathrm{K}}$ are compared in a Carnot cycle cooling hydrogen from 25 K to its boiling point of 20 K in a 5 T field. $Q_{20\mathrm{K}}$ for EuS is 1.9 J/cm^3. As for RM_2 compounds, $Q_{20\mathrm{K}}$ for $ErAl_2$ and $HoAl_2$ are 1.4 and 0.46 J/cm^3, respectively and that for $DyNi_2$ is almost the same as EuS [12, 13, 14]. As for garnet materials, $Q_{20\mathrm{K}}$ for GGG, $(Dy_{0.8}Gd_{0.2})_3Al_5O_{12}$ [4, 9], and $Gd_3(Ga_{0.6}Fe_{0.4})_5O_{12}$ (GGIG(40%)) [11] are 0.29, 0.51, and 0.25 J/cm^3, respectively. Comparing with these magnetic materials, EuS has higher cooling power per unit volume than RAl_2 compounds and especially several times higher than the garnet materials. In our previous tests of Carnot cycle magnetic refrigeration, plates of garnet materials were used for hydrogen liquefaction [4]. Because we can manufacture EuS into plates, the current results indicate that sintered EuS may improve the cooling power of Carnot magnetic liquefaction stage.

The AMR cycle is considered useful above 20 K, but numerical simulation is necessary to evaluate the cooling power in an AMR cycle [27, 28, 29]. Evaluation of sintered EuS using the AMR cycle is beyond the scope of this paper and will be discussed elsewhere.

5. Conclusions

A sintered compact of the ferromagnetic semiconductor EuS having a relative density larger than 95% was synthesized. The MCE is studied in the vicinity of its ordering temperature and is shown to be close to that of a single crystal. The S–T diagram of sintered EuS was obtained. The high magnetic entropy change and absorbed heat per unit volume near 20 K indicate that sintered EuS is potentially an excellent magnetic refrigerant for hydrogen liquefaction.

Acknowledgments

This work was partly supported by JSPS KAKENHI.

References

[1] Debye P. Einige Bemerkungen zur Magnetisierung bei tiefer Temperatur. Ann Physik 1926; 81: 1154.

[2] Giauque W.F. Paramagnetism and the third law of thermodynamics. Interpretation of the low-temperature magnetic susceptibility of gadolimium sulfate. J Am Chem Soc 1927; 49: 1870.

[3] Shirron PJ. Applications of the magnetocaloric effect in single-stage, multi-stage and continuous adiabatic demagnetization refrigerators. Cryogenics 62 (2014) 130-139.

[4] Numazawa T, Kamiya K, Utaki T, Matsumoto K. Magnetic refrigerator for hydrogen liquefaction. Cryogenics 2014; 62 : 185-192.

[5] Brown GV. Magnetic heat pumping near room temperature. J Appl Phys 1976;47:3673-80.

[6] Gschneidner jr KA, Pecharsky VK. Thirty years of near room temperature magnetic cooling: where we are today and future prospects. Int J Refriger 2008;31:945-61.

[7] Gschneidner Jr KA, Pecharsky VK, Tsokol AO. Recent developments in magnetocaloric materials. Rep Prog Phys 2005;68:1479-539.

[8] Tishin AM. Magnetocaloric effect: current situation and future trends. J Magn Magn Mater 2007;316:351-7.

[9] Numazawa T, Kamiya K, Abe S, Matsumoto K. Thermal and Mechanical Properties of Magnetic Materials for Carnot Magnetic Refrigeration on Hydrogen Liquefaction. Proc WHEC 2004;15.

[10] McMichael RD, Ritter JJ, Shull RD. Enhanced magnetocaloric effect in $Gd_3Ga_{5-x}Fe_xO_{12}$. J Appl Phys 1993;73:6946-6948.

[11] Matsumoto K, Matsuzaki A, Kamiya K, Numazawa T. Magnetocaloric effect, specific heat and entropy of iron-substituted gadolinium gallium garnets $Gd_3(Ga_{1-x}Fe_x)_5O_{12}$. Jpn J Appl Phys 2009;48:113002.

[12] Tomokiyo A, Yayama H, Wakabayashi H, Kuzuhara T, Hashimoto T, Sahashi M, et al. Specific heat and entropy of RNi_2 (R: rare earth heavy metals) in magnetic field. Adv Cryo Eng 1986;32:295-301.

[13] Hashimoto T, Matsumoto K, Kurihara T, Numazawa T, Tomokiyo A, Yayama H, Goto T, Todo S, Sahashi M. Investigation on the possibility of the RAl_2 system as a refrigerant in an Ericsson type magnetic refrigerator. Adv Cryo Eng Material 1986; 32: 279-286.

[14] Hashimoto T. Recent investigation on refrigerants for magnetic refrigerators. Adv Cryo Eng 1986;32:261-70.

[15] Zhu Y, Asamoto K, Nishimura Y, Kouen T, Abe S, Matsumoto K, Numazawa T. Magnetocaloric Effect of $(Er_xR_{1-x})Co_2$ (R = Ho, Dy) for Magnetic Refrigeration between 20 and 80 K. Cryogenics 2011;51:494-498.

[16] McGuire TR, Argyle BE, Shafer MW, Smart JS. Ferromagnetism in divalent Europium salts. Appl Phys Lett 1962; 1: 17.

[17] Li DX, Yamamura T, Nimori S, Homma Y, Honda F, Aoki D. Giant and isotropic low temperature magnetocaloric effect in magnetic semiconductor EuSe. Appl Phys Lett 2013; 102: 152409.

[18] Ahn K, Pecharsky AO, Gschneidner KA, Pecharsky VK. Preparation, heat capacity, magnetic properties, and the magnetocaloric effect of EuO. J Appl Phys 2004; 97 : 063901.

[19] Hashimoto T, Numasawa T, Shiino M, Okada T. Magnetic refrigeration in the temperature range from 10 K to room temperature: the ferromagnetic refrigerants. Cryogenics 1981; 21: 647-653.

[20] Ghosh PK, Dutta Roy SK. Magnetocaloric effect in some chalcogenide compounds at low temperatures. lnd J Pure Appl Phys 1985; 23: 362-365.

[21] Wood ME, Potter WH. General analysis of magnetic refrigeration and its optimization using a new concept: maximization of refrigerant capacity. Cryogenics 1985; 25: 667-683.

[22] Bredy P, Seyfert P. Measurement of magnetic field induced change in the entropy of europium sulphide. Cryogenics 1988; 28: 605.

[23] Li DX, Yamamura T, Nimori S, Homma Y, Honda F, Haga Y, Aoki D. Large reversible magnetocaloric effect in ferromagnetic semiconductor EuS. Solid State Communications 2014; 193 : 6-10

[24] Li L, Hirai S, Nakamura E, Yuan H. Synthesis of europium sulfides by CS_2 sulfurization and heat treatment. MRS Advances (in print)

[25] Gschneidner Jr. KA, Pecharsky VK, Magnetocaloric materials. Annu. Rev. Mater. Sci. 2000; 30: 387.

[26] Lorusso G, Sharples JW, Palacios E, Roubeau O, Brechin EK, Sessoli R, Rossin A, Tuna F, Mclnnes EJL, Collison D, Evangelisti M. A Dense Metal-Organic Framework for Enhanced Magnetic Refrigeration. Adv. Mater. 2013; 25: 4653.

[27] Matsumoto K, Hashimoto T. Thermodynamic analysis of magnetically active regenerator from 30 to 70K with a Brayton-like cycle. Cryogenics 1990;30:840-5.

[28] Matsumoto K, Kondo T, Ikeda M, Numazawa T. Numerical analysis of active magnetic regenerators for hydrogen magnetic refrigeration between 20 and 77 K. Cryogenics 2011; 51: 353-7.

[29] Park I, Kim Y, Park J, Jeong S. Design method of the layered active magnetic regenerator (AMR) for hydrogen liquefaction by numerical simulation Cryogenics 2015; 70 : 57-64